

Depolarizing-Field Effect in Strained Nanoscale Ferroelectric Capacitors and Tunnel Junctions

N. A. Pertsev and H. Kohlstedt

Institut für Festkörperforschung, Forschungszentrum Jülich, D-52425 Jülich, Germany

(cond-mat/0603762, version 2, 8 November 2006)

The influence of depolarizing field on the magnitude and stability of a uniform polarization in ferroelectric capacitors and tunnel junctions is studied using a nonlinear thermodynamic theory. It is predicted that, in heterostructures involving strained epitaxial films and metal electrodes, the homogeneous polarization state may remain stable against transformations into the paraelectric phase and into polydomain states down to the nanoscale. This result supports the possibility of depolarizing-field-related resistive switching in ferroelectric tunnel junctions with dissimilar electrodes. The resistance on/off ratio in such junctions is shown to be governed by the difference between the reciprocal capacitances of screening space charges in the electrodes.

I. INTRODUCTION

Persistence of ferroelectricity in ultrathin films is an issue of high fundamental and practical interest. In particular, the stability of ferroelectric states with a nonzero net polarization represents a matter of primary importance. Indeed, the presence of considerable remnant out-of-plane polarization is necessary for the memory applications of ferroelectric films in the form of capacitors [1] and ferroelectric tunnel junctions (FTJs) [2-4].

Dependence of the ferroelectric polarization \mathbf{P} on the thickness of a thin film sandwiched between two electrodes may result from both long-range and short-range interactions. The most widely discussed cause of this size effect is the existence of a depolarizing field appearing when the polarization charges $\rho = -\text{div } \mathbf{P}$ at the film surfaces are not perfectly compensated for by free charge carriers [5-11]. The phenomenological theory predicted long time ago that this internal electric field differs from zero even in thin films covered by metal electrodes [6,8]. The depolarizing-field effect may lead to the instability of the out-of-plane polarization in ultrathin films resulting in complete disappearance of ferroelectric phase below some critical thickness [5,7]. This prediction of the mean-field theory was supported recently by first-principles calculations [10,11]. The depolarizing-field effect on

polarization was invoked to explain gradual reduction of tetragonality measured in ultrathin PbTiO_3 films [12] and the time-dependent polarization relaxation observed in $\text{SrRuO}_3/\text{BaTiO}_3/\text{SrRuO}_3$ capacitors [13]. In addition to the long-range depolarizing field, the polarization in a thin film may be affected by the intrinsic surface effect associated with dipole-dipole interactions [14] and by short-range interactions between atomic layers adjacent to the ferroelectric-electrode interface [11].

In epitaxial films, which are most suited for the fabrication of ferroelectric capacitors and tunnel junctions, the polarization state is also strongly influenced by lattice strains induced by the mechanical film/substrate interaction [15,16]. Fortunately, the out-of-plane polarization is enhanced in epitaxial films of perovskite ferroelectrics grown on “compressive” substrates [17]. In this case the electrostrictive coupling between the polarization and compressive in-plane strains makes the out-of-plane polarization state more stable than in free standing films [18]. Accordingly, in epitaxial films grown on compressive substrates the depolarizing-field effect competes with the lattice-strain one. This competition must be taken into account in the studies of strained ferroelectric capacitors and FTJs.

The aim of this paper is to analyze the influence of depolarizing field on the physical properties of strained ferroelectric films sandwiched between metallic electrodes. In contrast to some recent studies [4,13], we use a nonlinear thermodynamic theory to calculate the depolarizing field and the film polarization in a metal-ferroelectric-metal (MFM) heterostructure self-consistently. The results of our calculations indicate that the nanoscale ferroelectric capacitors and FTJs can be employed for memory applications.

We focus on thin films of perovskite ferroelectrics epitaxially grown on a thick cubic substrate inducing compressive in-plane lattice strains in the film. At thicknesses outside the nanoscale range, such films stabilize in the tetragonal c phase with the polarization orthogonal to the film surfaces [15,16]. Since we are interested in the memory applications, the c phase is taken to be in a single-domain state. (This is an appropriate model because an electric field larger than the coercive field is applied to the film in a memory cell so that the 180° domains are mostly removed.) Neglecting for clarity the surface effects on polarization [11,14] and a weak conductivity of perovskite ferroelectrics at low temperatures, we can further assume the film to be homogeneously polarized. For such ferroelectric film, we first calculate the equilibrium polarization as a function of the film thickness and then determine the thickness range, where the single-domain state is stable with respect to the transformation into a polydomain one. It should be noted that in some part of this range the uniformly polarized state may appear to be energetically less favorable than the 180° domain pattern [19,20]. Such metastability, however, is not detrimental for memory applications, provided that the potential barrier between the aforementioned states is high enough to prevent fast relaxation of the remanent polarization at a low operating temperature.

II. THICKNESS DEPENDENCE OF SPONTANEOUS POLARIZATION

To calculate the equilibrium polarization, we use a nonlinear equation of state of a strained ferroelectric film.

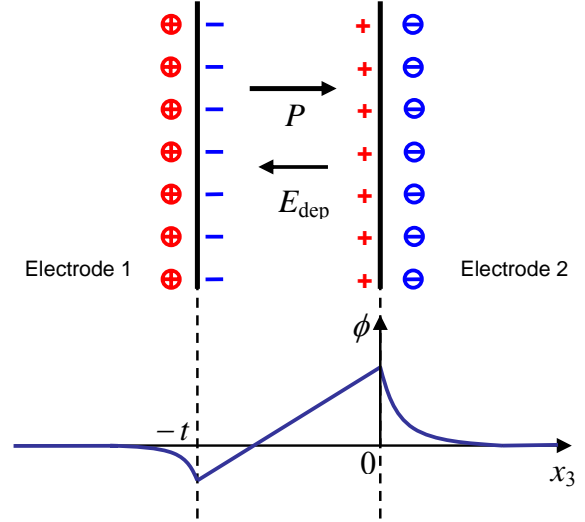


FIG. 1. Screening of polarization charges in a metal-ferroelectric-metal heterostructure. Distribution of the electrostatic potential ϕ is shown schematically for the case of dissimilar electrodes kept at a bias voltage compensating for the difference of their work functions.

Such equation can be derived by differentiating the film thermodynamic potential [15,16] or the Helmholtz free energy [17] written in terms of polarization components P_i ($i = 1, 2, 3$). For the c phase ($P_1 = P_2 = 0, P_3 \neq 0$) stable at negative misfit strains S_m , the relevant equation reduces to

$$2a_3^*P_3 + 4a_{33}^*P_3^3 + 6a_{111}P_3^5 + 8a_{1111}P_3^7 + \dots = E_3, \quad (1)$$

where $a_3^* = a_1 + 2S_m(q_{11}c_{12} - q_{12}c_{11})/c_{11}$, $a_{33}^* = a_{11} - q_{11}^2/(2c_{11})$, a_1 , a_{ij} , a_{ijk} , and a_{ijkl} are the dielectric stiffness coefficients at constant strain, q_{ln} are the relevant electrostrictive constants, and c_{ln} are the film elastic stiffnesses at constant polarization. The field E_3 inside the film can be calculated from the total voltage drop across the MFM heterostructure and the continuity condition of the electric displacement $\mathbf{D} = \epsilon_0 \mathbf{E} + \mathbf{P}$ at the ferroelectric-metal interfaces (ϵ_0 is the permittivity of the vacuum) [6,7]. This procedure was employed in many papers, but the linear approximation was frequently used for the field dependence of the ferroelectric polarization [3,4,8,13]. In our formulation, the screening of polarization charges results from changes of the electron density inside the

electrodes. The electric field E_m in a metal electrode can be evaluated in the Thomas-Fermi approximation [21] corrected for the dielectric response of metallic lattice [22]. For a thick electrode occupying the space $x_3 \geq 0$ (see Fig. 1), the calculation gives [8]

$$E_m(x_3) = E_m(x_3 = 0) \exp(-x_3/l_s). \quad (2)$$

Here l_s is the screening length defined by the relation

$$l_s^2 = \left(\frac{3}{8\pi}\right)^{2/3} \frac{h^2 \varepsilon_0 \varepsilon_m}{3 e^2 m^* n_0^{1/3}}, \quad (3)$$

where n_0 is the mean electron density at zero electric field, ε_m is the relative permittivity of the ionic lattice in the metal, e is the electronic charge, m^* is the electron effective mass in the electrode, and h is the Planck constant. The field E_m at the boundary $x_3 = 0$ between the electrode and ferroelectric can be found from the electric displacement $D_m = \varepsilon_0 \varepsilon_m E_m$ in the metal, taking into account that $D_m(x_3 = 0)$ is defined by the total screening charge ρ_m in the electrode (per unit area). The integration of Eq. (2) then enables us to calculate the voltage change across the electrode to be $\Delta\phi_m = \rho_m l_s / (\varepsilon_0 \varepsilon_m)$. Introducing the capacitance c_m per unit area of the screening space charge [23,24] as $c_m = \varepsilon_0 \varepsilon_m / l_s$, we can write this relation in the compact form $\Delta\phi_m = \rho_m / c_m$.

The algebraic sum of the voltage drop $\Delta\phi_f = -E_3 t$ in a ferroelectric film of thickness t and the voltage changes $\Delta\phi_{m1} = -\rho_{m1} / c_{m1}$ and $\Delta\phi_{m2} = \rho_{m2} / c_{m2}$ in the left and right electrodes is governed by the applied voltage difference $V_a = V_2 - V_1$. The continuity of electrostatic potential yields

$$V_a = -\frac{\rho_{m1}}{c_{m1}} - E_3 t + \frac{\rho_{m2}}{c_{m2}} + \frac{W_2 - W_1}{e}, \quad (4)$$

where the last term accounts for the contact potential difference that appears when electrodes have different work functions W_1 and W_2 [25]. For the screening charges ρ_{m1} and ρ_{m2} , the boundary conditions at the two

ferroelectric/electrode interfaces give $\rho_{m1} = \varepsilon_0 E_3 + P_3$ and $\rho_{m2} = -(\varepsilon_0 E_3 + P_3)$. Substituting these relations into Eq. (4), we finally obtain the formula

$$E_3 = -\frac{P_3}{\varepsilon_0 + c_i t} - \frac{c_i}{(\varepsilon_0 + c_i t)} \left(V_a - \frac{W_2 - W_1}{e} \right) \quad (5)$$

for the total field inside the film [26]. The first term in Eq. (5), which is proportional to the film out-of-plane polarization, represents the depolarizing field E_{dep} . It can be seen that the only parameter of the electrodes that directly affects E_{dep} is the *total interfacial capacitance* $c_i = (c_{m1}^{-1} + c_{m2}^{-1})^{-1}$ resulting from the presence of two capacitances c_{m1} and c_{m2} in series. Existence of an interfacial capacitance c_i also reduces the second term in Eq. (5), which describes the external field acting on a ferroelectric film. However, this reduction is expected to be weak since usually $c_i t \gg \varepsilon_0$.

The substitution of Eq. (5) into Eq. (1) shows that the depolarizing field formally renormalizes the coefficient a_3^* of the lowest-order polarization term. This renormalization, which can be described by the introduction of the coefficient

$$a_3^{**} = a_3^* + \frac{1}{2(\varepsilon_0 + c_i t)} = a_1 + 2 \left(\frac{q_{11} c_{12}}{c_{11}} - q_{12} \right) S_m + \frac{1}{2(\varepsilon_0 + c_i t)} \quad (6)$$

instead of a_3^* , should affect all physical properties of a single-domain ferroelectric film. However, the difference between the coefficients a_3^{**} and a_1 may be reduced and even compensated by the strain effect. Indeed, the second term on the right-hand side of Eq. (6) is negative for films of perovskite ferroelectrics grown on an appropriate compressive substrate ($S_m < 0$), and large strain magnitudes may be achieved when the critical thickness for the generation of misfit dislocations is not exceeded. Hence the depolarizing-field-induced increase of a_3^{**} can be compensated down to the film thickness $t^* \cong c_{11} / [4(q_{11} c_{12} - q_{12} c_{11})(-S_m) c_i]$.

Using Eqs. (1) and (5), we can calculate the out-of-plane polarization and depolarizing field as a function of the film thickness at a constant misfit strain $S_m < 0$. In symmetric MFM heterostructures ($W_1 = W_2$), the spontaneous polarization $P_s = P_3(V_a = 0)$ is progressively suppressed in thinner films due to the depolarizing-field effect. For perovskite ferroelectrics, the coefficient a_{33}^* involved in Eq. (1) is positive so that we may first evaluate $P_s(t)$ in the P^4 approximation. The calculation yields

$$P_s^2 = \frac{1}{2a_{33}^*} \left[\frac{\theta - T}{2\varepsilon_0 C} - 2 \left(\frac{q_{11}c_{12}}{c_{11}} - q_{12} \right) S_m - \frac{1}{2(\varepsilon_0 + c_i t)} \right], \quad (7)$$

where θ and C are the Curie-Weiss temperature and constant of the bulk ferroelectric crystal. Equation (7) shows that the strain effect shifts the polarization suppression to smaller film thicknesses. At a fixed temperature T , the out-of-plane polarization P_s vanishes below a critical film thickness t_0 , which was regarded as a size-induced phase transition [10,27]. From Eq. (7) it follows that t_0 is inversely proportional to the interfacial capacitance, being given by the formula

$$t_0 \cong \frac{1}{c_i} \left[\frac{\theta - T}{\varepsilon_0 C} - 4 \left(\frac{q_{11}c_{12}}{c_{11}} - q_{12} \right) S_m \right]^{-1}. \quad (8)$$

It should be emphasized, however, that this expression for the thickness t_0 is valid only at temperatures $T > T_1 = \theta + 2\varepsilon_0 C (q_{11} + q_{12} - 2q_{12}c_{12}/c_{11})S_m$, where the ferroelectric c phase transforms below t_0 into the paraelectric phase. The calculations show that at $T < T_1$ the depolarizing field leads to the *polarization rotation*, but not to the disappearance of ferroelectricity at $t < t_0$. Instead of the paraelectric phase, an in-plane polarization state ($P_1 \neq 0$, $P_2 \neq 0$, $P_3 = 0$) becomes stable in thinnest films, e.g., the aa phase in the single-domain case [15]. The critical thickness $t_0(T < T_1)$ is larger than t_0 given by Eq. (8) since the transition is of the first-order at $T < T_1$. This kind of thickness-induced phase transformation was not considered in the preceding publications [10,11,27], where only

complete disappearance of ferroelectricity below t_0 was discussed.

At film thicknesses well above $t_0(T)$, the spontaneous polarization $P_s(t)$ should be calculated from Eq. (1) using the P^6 or higher-order approximation. We performed these calculations for $\text{Pb}(\text{Zr}_{0.5}\text{Ti}_{0.5})\text{O}_3$ and BaTiO_3 films grown on SrTiO_3 , assuming the misfit strain S_m to be equal to a thickness-independent value attained in fully strained MFM trilayers. For $\text{Pb}(\text{Zr}_{0.5}\text{Ti}_{0.5})\text{O}_3$ films, we employed the P^6 approximation with the material parameters [28] determined from the set used in Ref. 16. The polarization of BaTiO_3 films was calculated in the P^8 approximation using the thermodynamic parameters of BaTiO_3 obtained recently in Ref. [29] and the elastic and electrostrictive constants of this crystal [30]. Since the magnitude of the interfacial capacitance c_i affects the spontaneous polarization only via the product $c_i t$, the dependences $P_s(t)$ corresponding to different electrode materials can be described by one universal curve $P_s(t_{\text{eff}})$. Here the effective film thickness t_{eff} is directly proportional to the actual thickness t and may be defined as $t_{\text{eff}} = (c_i/c_1)t$, where $c_1 = 1 \text{ F/m}^2$.

The dependences $P_s(t_{\text{eff}})$ calculated for strained $\text{Pb}(\text{Zr}_{0.5}\text{Ti}_{0.5})\text{O}_3$ and BaTiO_3 films are shown in Fig. 2. It can be seen that just above t_0 the spontaneous polarization steeply increases with thickness and reaches values comparable to the bulk polarization. At $c_i = 0.444 \text{ F/m}^2$ characteristic of SrRuO_3 electrodes [13], for example, Eq. (8) gives $t_0 \cong 2 \text{ nm}$ for $\text{Pb}(\text{Zr}_{0.5}\text{Ti}_{0.5})\text{O}_3$ films and $t_0 \cong 2.6 \text{ nm}$ for BaTiO_3 films. Therefore, even nanoscale capacitors and tunnel junctions may have the out-of-plane polarization sufficient for the memory applications.

From Eqs. (1) and (5) we can also calculate the thickness dependence of the depolarizing field, which is described by a universal curve $E_{\text{dep}}(t_{\text{eff}})$. Figure 2 demonstrates that E_{dep} varies nonmonotonically with the film thickness, reaching maximum at some thickness above t_0 . Remarkably, the maximum value of E_{dep} is independent of the interfacial capacitance c_i . Comparing this value with the electric field $E_g = \Delta_g/(et)$ necessary for the generation of free carriers inside a ferroelectric

having the band gap Δ_g [6], we can check the validity of our assumption that ferroelectric behaves as an insulator. For BaTiO_3 and $\text{Pb}(\text{Zr}_{0.5}\text{Ti}_{0.5})\text{O}_3$, the band gap is about 3.5 eV so that in the discussed nanoscale range E_g appears to be much larger than E_{dep} [E_g reduces below the maximum depolarizing field only at film thicknesses larger than 19 nm for BaTiO_3 and 9 nm for $\text{Pb}(\text{Zr}_{0.5}\text{Ti}_{0.5})\text{O}_3$].

III. STABILITY OF SINGLE-DOMAIN STATE

Now we must investigate the stability of single-domain polarization state against the formation of a 180° domain pattern reducing the depolarizing field inside the film. To that end, it is necessary to analyze a wave-like perturbation of the uniform polarization state [31]. In contrast to the previous simplified treatments of similar stability problems [31,32,20], we present a rigorous formulation of the problem for perovskite ferroelectrics.

Since the polarization distribution becomes inhomogeneous, the equation of state (1) should be replaced by the Euler equations involving the gradient terms. For ferroelectrics with a cubic paraelectric phase, these equations in our two-dimensional case [33] become

$$\begin{aligned} & (2a_1 + 4a_{11}P_1^2 + 2a_{12}P_3^2 + \dots)P_1 - 2q_{11}S_{11}P_1 \\ & - 2q_{12}(S_{22} + S_{33})P_1 - 2q_{44}S_{13}P_3 - E_1 \\ & = g_{11}P_{1,11} + g_{44}P_{1,33} + (g_{12} + g_{44})P_{3,13}, \end{aligned} \quad (9)$$

$$\begin{aligned} & (2a_1 + 4a_{11}P_3^2 + 2a_{12}P_1^2 + \dots)P_3 - 2q_{11}S_{33}P_3 \\ & - 2q_{12}(S_{11} + S_{22})P_3 - 2q_{44}S_{13}P_1 - E_3 \\ & = (g_{12} + g_{44})P_{1,13} + g_{44}P_{3,11} + g_{11}P_{3,33}, \end{aligned} \quad (10)$$

where indices after the comma denote differentiation with respect to the coordinates x_1 and x_3 , g_{ln} are the coefficients of the gradient terms in the free-energy expansion [34], and S_{ij} are the lattice strains in the film ($S_{22} = S_m$).

The polarization components involved in Eqs. (9)-(10) can be written as $P_3 = P_s + \delta P_3(x_3) \exp(ikx_1)$ and $P_1 = \delta P_1(x_3) \exp(ikx_1)$ with $\delta P_1, \delta P_3 \ll P_s$. Similar relations $S_{33} = (q_{11}P_s^2 - 2c_{12}S_m)/c_{11} + \delta S_{33}(x_3) \exp(ikx_1)$, $S_{11} = S_m + \delta S_{11}(x_3) \exp(ikx_1)$, $S_{13} = \delta S_{13}(x_3) \exp(ikx_1)$,

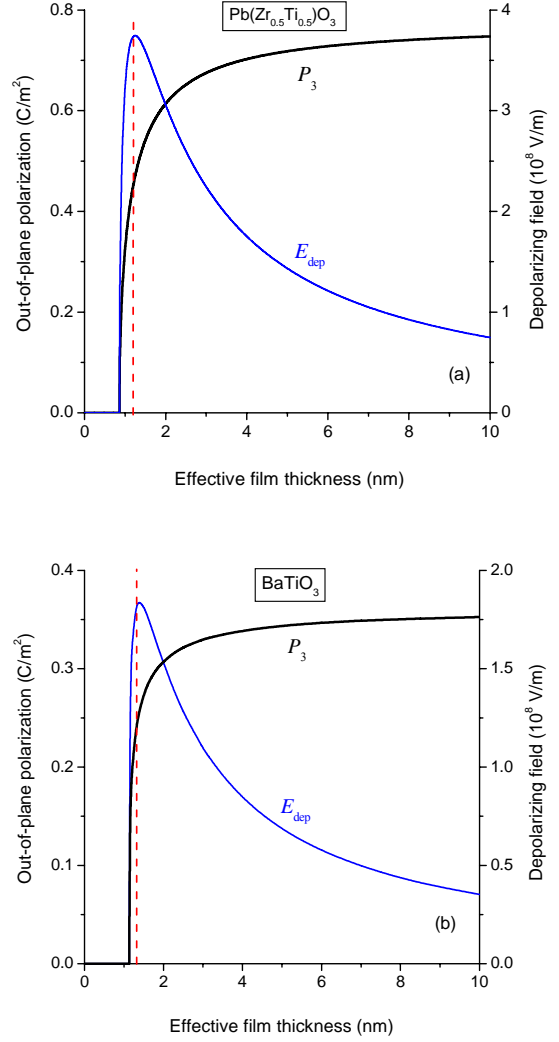


FIG. 2. Thickness dependence of the out-of-plane polarization and depolarizing field in ultrathin $\text{Pb}(\text{Zr}_{0.5}\text{Ti}_{0.5})\text{O}_3$ (a) and BaTiO_3 (b) films epitaxially grown on SrTiO_3 . The misfit strain is taken to be -26×10^{-3} for BaTiO_3 films [17] and -39×10^{-3} for $\text{Pb}(\text{Zr}_{0.5}\text{Ti}_{0.5})\text{O}_3$ films [18]; the temperature equals 25 °C. The actual film thickness t corresponding to a given effective thickness t_{eff} can be found from the relation $t = (c_1/c_i) t_{\text{eff}}$, where $c_1 = 1 \text{ F/m}^2$ and c_i is the total capacitance of the electrodes. The dashed line shows the film thickness below which the single-domain state becomes unstable.

and $\phi = \phi_0(x_3) + \delta\phi(x_3) \exp(ikx_1)$ can be introduced for the film strains and the electrostatic potential ϕ . Using these formulae and retaining only the lowest-order perturbation terms, we obtain

$$\begin{aligned} & (\tilde{\chi}_{11} + g_{11}k^2)\delta P_1 - 2q_{44}P_s\delta S_{13} + ik\delta\phi \\ & = g_{44}\delta P_{1,33} + ik(g_{12} + g_{44})\delta P_{3,3}, \end{aligned} \quad (11)$$

$$\begin{aligned} & (\tilde{\chi}_{33} + g_{44}k^2)\delta P_3 - 2q_{11}P_s\delta S_{33} - 2q_{12}P_s\delta S_{11} + \delta\phi_{,3} \\ & = ik(g_{12} + g_{44})\delta P_{1,3} + g_{11}\delta P_{3,33}, \end{aligned} \quad (12)$$

where $\tilde{\chi}_{11} = 2a_1 - 2(q_{11} + q_{12} - 2q_{12}c_{12}/c_{11})S_m + 2(a_{12} - q_{11}q_{12}/c_{11})P_s^2 + 2a_{112}P_s^4 + \dots$ and $\tilde{\chi}_{33} = 2a_1 + 4[q_{11}(c_{12}/c_{11}) - q_{12}]S_m + 12[a_{11} - q_{11}^2/(6c_{11})]P_s^2 + 30a_{111}P_s^4 + \dots$. It should be noted that $\tilde{\chi}_{11}$ and $\tilde{\chi}_{33}$ depend on the interfacial capacitance c_i and the film thickness t because the spontaneous polarization P_s is a function of these parameters.

In addition to Eqs. (11)-(12), several other relationships must be satisfied. First, the electrostatic condition $\text{div } \mathbf{D} = 0$ holding inside an insulating film yields the following relation between the perturbation $\delta\phi$ of electrostatic potential and the polarization perturbations:

$$ik\delta P_1 + \delta P_{3,3} + \varepsilon_0(k^2\delta\phi - \delta\phi_{,33}) = 0. \quad (13)$$

Second, the strains S_{ij} in the film must obey the classical compatibility condition $e_{ikl}e_{jmn}S_{m,km} = 0$, where e_{ikl} is the permutation symbol. In our case, this condition reduces to

$$\delta S_{11,33} - k^2\delta S_{33} = 2ik\delta S_{13,3}. \quad (14)$$

Finally, from the equations of mechanical equilibrium $\sigma_{ij,j} = 0$ written for the stresses σ_{ij} in the film we obtain

$$ik(c_{11}\delta S_{11} + c_{12}\delta S_{33}) + 4c_{44}\delta S_{13,3} = 2q_{44}P_s\delta P_{1,3} + 2ikq_{12}P_s\delta P_3, \quad (15)$$

$$c_{12}\delta S_{11,3} + c_{11}\delta S_{33,3} + 4ikc_{44}\delta S_{13} = 2ikq_{44}P_s\delta P_1 + 2q_{11}P_s\delta P_{3,3}. \quad (16)$$

Equations (11)-(16) form a system of six differential equations for six unknown functions: δP_1 , δP_3 , $\delta\phi$, δS_{11} , δS_{33} , and δS_{13} . The analysis of this system shows that the terms involving very small factor ε_0 may be neglected in

comparison with other terms. Then, after some mathematical manipulation, Eqs. (11)-(16) may be reduced to the following system of two simultaneous equations:

$$\begin{aligned} & \left[\tilde{\chi}_{33} - 2q_{12} \frac{(2q_{11} - q_{44})}{(c_{12} + 2c_{44})} P_s^2 + g_{44}k^2 \right] k^2 \delta P_3 \\ & - \left[\tilde{\chi}_{11} + 2q_{44} \frac{(2q_{11} - q_{44})}{(c_{12} + 2c_{44})} P_s^2 + 2(g_{11} - g_{12} - g_{44})k^2 \right] \delta P_{3,33} \\ & + g_{44}\delta P_{3,3333} - \left[2q_{12} - c_{11} \frac{(2q_{11} - q_{44})}{(c_{12} + 2c_{44})} \right] P_s k^2 \delta S_{11} \\ & - \left[q_{44} + 2c_{44} \frac{(2q_{11} - q_{44})}{(c_{12} + 2c_{44})} \right] P_s \delta S_{11,33} = 0, \end{aligned} \quad (17)$$

$$\begin{aligned} & 4c_{44}q_{12}P_s k^4 \delta P_3 + 2[(c_{12} + 2c_{44})q_{11} - c_{11}q_{12} - c_{12}q_{44}] \\ & \times P_s k^2 \delta P_{3,33} - 2c_{11}q_{44}P_s \delta P_{3,3333} - 2c_{11}c_{44}k^4 \delta S_{11} \\ & + (c_{11}^2 - c_{12}^2 - 4c_{12}c_{44})k^2 \delta S_{11,33} - 2c_{11}c_{44}\delta S_{11,3333} = 0. \end{aligned} \quad (18)$$

It should be emphasized that Eqs. (17)-(18) differ dramatically from the differential equation used to describe the stability of a uniform polarization state formerly [31,20]. Indeed, owing to the electrostrictive coupling between the polarization and strain, Eq. (17) contains terms depending on the lattice strain and its second derivative, which were totally ignored previously. Moreover, additional Eq. (18) must be satisfied because the polarization wave creates an elastic wave in a piezoelectric medium.

Since the system (17)-(18) is homogeneous, we may seek the solution in the form of $\delta P_3 = A \exp(\lambda x_3)$ and $\delta S_{11} = B \exp(\lambda x_3)$. The substitution of these formulae into Eqs. (17)-(18) leads to a homogeneous system of two linear algebraic equations in the unknown coefficients A and B . Calculating the determinant Δ_λ of this system and setting it to zero, we obtain the characteristic equation $\Delta_\lambda(\lambda) = 0$ being a quartic algebraic equation with respect to λ^2 in our case. When all roots $\lambda_n(k)$ of this equation are distinct, the sought perturbations can be written as $\delta P_3 = \sum_{n=1}^8 A_n \exp(\lambda_n x_3)$ and $\delta S_{11} = \sum_{n=1}^8 B_n \exp(\lambda_n x_3)$. Here each coefficient B_n can be expressed in terms of A_n using Eq. (18), for example. The calculation yields

$$B_n = 2P_s A_n \times \frac{2c_{44}q_{12}k^4 + [(c_{12} + 2c_{44})q_{11} - c_{11}q_{12} - c_{12}q_{44}]k^2\lambda_n^2 - c_{11}q_{44}\lambda_n^4}{2c_{11}c_{44}k^4 - (c_{11}^2 - c_{12}^2 - 4c_{12}c_{44})k^2\lambda_n^2 + 2c_{11}c_{44}\lambda_n^4} \quad (19)$$

In turn, the coefficients A_n must satisfy a system of eight simultaneous equations, which follow from the boundary conditions on the problem.

To derive this system of equations, we first employ the continuity of potential ϕ and electric displacement D_3 at the film-electrode interfaces. Within the film, the variation $\delta\phi(x_3)$ of electrostatic potential can be calculated in terms of A_n using Eqs. (11)-(16). The potential ϕ_m inside the electrodes in the presence of polarization wave becomes $\phi_m = \phi_{m0}(x_3) + \delta\phi_m(x_3)\exp(ikx_1)$. The perturbation $\delta\phi_m(x_3)$ can be easily found in the screening length approximation to be $\delta\phi_m = L_2 \exp(-\zeta x_3)$ with $\zeta = \sqrt{k^2 + l_s^{-2}}$ in the right electrode ($x_3 \geq 0$) and $\delta\phi_m = L_1 \exp[\zeta(x_3 + t)]$ in the left one ($x_3 \leq -t$). Using these expressions to formulate the boundary conditions and eliminating then the constants L_1 and L_2 , we obtain $\delta P_3(x_3 = 0) = \varepsilon_0 \varepsilon_m \zeta \delta\phi(x_3 = 0)$ and $\delta P_3(x_3 = -t) = -\varepsilon_0 \varepsilon_m \zeta \delta\phi(x_3 = -t)$. These relationships give us the first two equations for A_n . Another two equations follow from the conditions imposed on the polarization derivative $P_{3,3}$ [14], which in the approximation of an infinite extrapolation length reduce to $\delta P_{3,3} = 0$ at $x_3 = 0$ and $x_3 = -t$.

Proceed now to the mechanical boundary conditions imposed on an epitaxial thin film grown on a nonpiezoelectric cubic substrate. Assuming the bottom electrode to be fully strained by a thick substrate, we shall neglect the mechanical influence of electrodes in comparison with the substrate effect. Then the conditions on the top film surface reduce to the absence of stresses σ_{33} and σ_{13} at $x_3 = 0$. The lattice matching on the bottom film surface implies the continuity of the mechanical displacement and the stresses σ_{33} and σ_{13} at $x_3 = -t$. It can be shown that the first of these conditions in our case gives

$$\begin{aligned} \delta S_{11} &= \delta S_{11}^{sub} \quad \text{and} \quad 2\delta S_{13} - (1/ik)\delta S_{11,3} = \\ &= 2\delta S_{13}^{sub} - (1/ik)\delta S_{11,3}^{sub} \quad \text{at} \quad x_3 = -t. \quad \text{The strains} \\ S_{ij}^{sub} &= \delta S_{ij}^{sub}(x_3)\exp(ikx_1) \quad \text{and} \quad \text{the stresses} \\ \sigma_{ij}^{sub} &= \delta\sigma_{ij}^{sub}(x_3)\exp(ikx_1) \quad \text{in the substrate can be} \end{aligned}$$

calculated from the compatibility condition and the equations of mechanical equilibrium. For the nonzero strains, the calculation gives

$$\delta S_{11}^{sub} = R_1 \exp(\beta_1 k x_3) + R_2 \exp(\beta_2 k x_3), \quad (20)$$

$$\begin{aligned} \delta S_{33}^{sub} &= -\frac{(c_{11} - 2c_{44}\beta_1^2)}{(c_{12} + 2c_{44})} R_1 \exp(\beta_1 k x_3) \\ &- \frac{(c_{11} - 2c_{44}\beta_2^2)}{(c_{12} + 2c_{44})} R_2 \exp(\beta_2 k x_3), \end{aligned} \quad (21)$$

$$\begin{aligned} \delta S_{13}^{sub} &= \frac{1}{4ic_{44}} \left\{ \left[\frac{c_{11}(c_{11} - 2c_{44}\beta_1^2)}{c_{12} + 2c_{44}} - c_{12} \right] \beta_1 R_1 \exp(\beta_1 k x_3) \right. \\ &\left. + \left[\frac{c_{11}(c_{11} - 2c_{44}\beta_2^2)}{c_{12} + 2c_{44}} - c_{12} \right] \beta_2 R_2 \exp(\beta_2 k x_3) \right\}, \end{aligned} \quad (22)$$

where $\beta_{1,2} = \sqrt{\xi \pm \sqrt{\xi^2 - 1}}$, $\xi = (c_{11}^2 - c_{12}^2 - 4c_{12}c_{44})/(4c_{11}c_{44})$ and c_{mm} are the elastic stiffnesses of the substrate assumed to be equal to the film stiffnesses for simplicity. Similar relations can be derived for the functions $\delta\sigma_{ij}^{sub}(x_3)$ defining the stresses in the substrate. The coefficients R_1 and R_2 represent additional unknown quantities which can be calculated in terms of A_n using the strain conditions on the film/substrate interface. The remaining four stress conditions together with the four electrical conditions give us the sought system of eight linear algebraic equations for the constants A_n .

Since this system is homogeneous, a nonzero solution for the set of coefficients A_n exists only if the determinant Δ_A of this system equals zero. By solving the equation $\Delta_A(k) = 0$ numerically, it is possible to check the existence of any root $k \neq 0$ at a given film thickness t , interfacial capacitance c_i , temperature T , and misfit strain S_m . If there are no such roots, the uniform polarization state remains stable against inhomogeneous polarization perturbations.

The critical thickness t_c , at which the single-domain state becomes unstable, can be found as a maximum value of t at which a nonzero solution for k first appears.

We performed necessary numerical calculations for fully strained BaTiO_3 and $\text{Pb}(\text{Zr}_{0.5}\text{Ti}_{0.5})\text{O}_3$ films grown on SrTiO_3 . Since for our purposes it is sufficient to determine the upper bound $t_{c,\text{max}}$ of the critical thickness, we simplified the problem by setting the gradient coefficients g_m to zero. (Note that the polarization gradient terms can only decrease the critical thickness and that the values of g_m are not exactly known for perovskite ferroelectrics). Then the characteristic equation $\Delta_\lambda(\lambda) = 0$ reduces to a cubic equation with respect to λ^2 , and the roots λ_n of this equation become proportional to the wave number k .

Since the critical thickness is inversely proportional to the interfacial capacitance c_i , it is sufficient to compute $t_{c,\text{max}}$ for one particular value of c_i only. We studied the case of capacitors with two SrRuO_3 electrodes assuming $c_i = 0.444 \text{ F/m}^2$ [35]. At room temperature, $t_{c,\text{max}}$ was found to be slightly below 2.98 nm for BaTiO_3 films and below 2.73 nm for $\text{Pb}(\text{Zr}_{0.5}\text{Ti}_{0.5})\text{O}_3$ films. The magnitude of $t_{c,\text{max}}$ weakly decreases with decreasing temperature, reducing down to about 2.46 nm in BaTiO_3 films and to about 2.63 nm in $\text{Pb}(\text{Zr}_{0.5}\text{Ti}_{0.5})\text{O}_3$ films at $T = -200 \text{ }^\circ\text{C}$. The dependence of $t_{c,\text{max}}$ on the interfacial capacitance c_i at $T = 25 \text{ }^\circ\text{C}$ is shown in Fig. 3.

Our numerical calculations also demonstrated that the critical thickness t_c is always smaller than the thickness t_{th} at which the film inverse susceptibility $\chi_{33} = 2a_3^* + 12a_{33}^*P_s^2 + 30a_{111}P_s^4 + \dots$ goes to zero. Since the ‘‘threshold’’ thickness t_{th} becomes very close to t_c when the latter corresponds to the nanoscale range [at room temperature, $t_{th} \cong 3.1 \text{ nm}$ for BaTiO_3 films and $t_{th} \cong 2.81 \text{ nm}$ for $\text{Pb}(\text{Zr}_{0.5}\text{Ti}_{0.5})\text{O}_3$ films], the equation $\chi_{33}(t) = 0$ may be used to roughly estimate the upper bound of t_c without performing complicated numerical calculations.

Thus, by combining highly strained epitaxial films with metallic electrodes having good screening properties it is possible to stabilize the single-domain ferroelectric state in nanoscale capacitors and tunnel junctions [36].

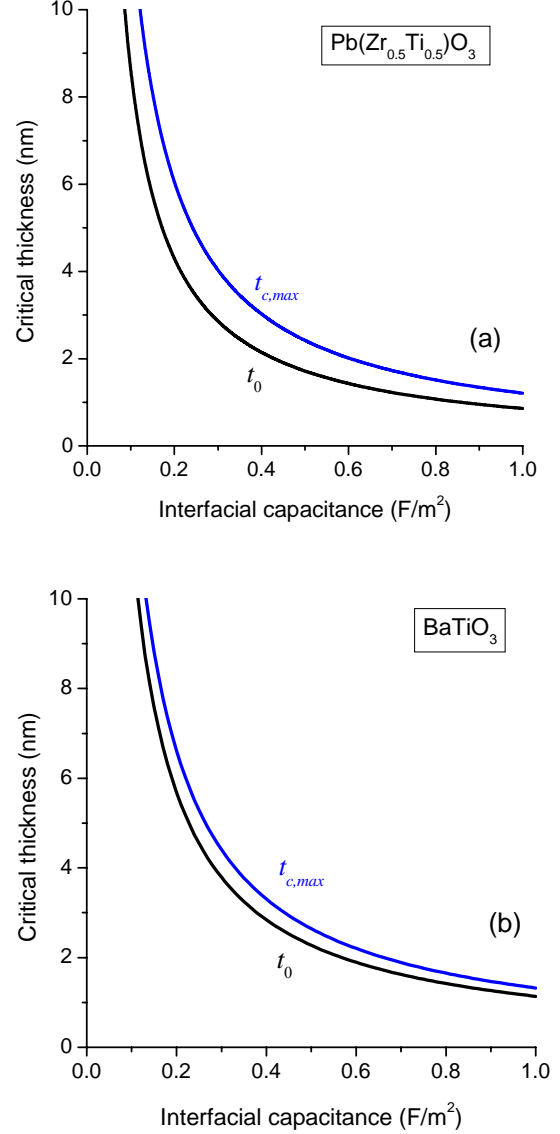


FIG. 3. Critical thicknesses of strained $\text{Pb}(\text{Zr}_{0.5}\text{Ti}_{0.5})\text{O}_3$ (a) and BaTiO_3 (b) films as a function of the total interfacial capacitance characterizing the screening space charge in the electrodes. Here t_0 is the thickness at which the out-of-plane polarization goes to zero, and $t_{c,\text{max}}$ is the upper bound of the critical thickness below which the single-domain c phase becomes unstable with respect to the formation of 180° domains.

Remarkably, this stabilization results from the elastic effect caused by the electrostrictive coupling between polarization and strain, which was totally ignored previously [31,20].

IV. DEPOLARIZING-FIELD EFFECT ON ELECTRON TUNNELING

Proceed now to the asymmetric MFM heterostructures that involve dissimilar electrodes. When the electrode work functions W_1 and W_2 are different, a nonzero electric field $E_3 \cong (W_2 - W_1)/(et)$ acts on the film in a short-circuited capacitor [25]. This field increases with decreasing film thickness and becomes very strong in ultrathin films. In the case of one SrRuO₃ and one Pt electrode, for example, we have $W_1 \approx 5.2$ eV [37] and $W_2 \approx 5.65$ eV [38] so that the field intensity exceeds 10^8 V/m at $t < 4.5$ nm. Evidently, the film becomes homogeneously polarized under such field, with the polarization pointing to the electrode having higher work function. Since this polarization is only weakly dependent on temperature, the ferroelectric to paraelectric transition disappears in a film sandwiched between short-circuited dissimilar electrodes.

The usual temperature dependence of polarization, however, restores when a bias voltage $V_a = (W_1 - W_2)/e$ is applied to the electrodes. Hence the plots shown in Fig. 2 now describe the thickness dependence of the polarization $P_3(V_a)$ appearing at this voltage. The polarization reversal also occurs in asymmetric capacitors, but the hysteresis loop becomes shifted along the voltage axis.

Another specific feature of asymmetric MFM heterostructures is associated with the screening of polarization charges by dissimilar electrodes. When the screening abilities of two electrodes are different, the depolarizing field changes the *mean value* of electrostatic potential in the heterostructure [3,4]. This feature is expected to play an important role in ferroelectric tunnel junctions (FTJs), where the quantum mechanical electron tunneling represents the dominant conduction mechanism. Indeed, since the sign of the above effect depends on the polarization orientation in the ferroelectric barrier, the polarization reversal occurring at the coercive voltage V_c should be accompanied by a change of the barrier conductance. Such a resistive switching of ferroelectric origin was studied theoretically in Refs. [3,4], but a linear approximation was employed for the field dependence of polarization.

The nonlinear theory enables us to calculate the depolarizing-field-induced change $\Delta\bar{\phi}$ of the mean potential $\bar{\phi}$ in the ferroelectric barrier rigorously. Since in our case $\bar{\phi}$ is equal to the arithmetic mean of electrostatic potentials on the film surfaces, $\Delta\bar{\phi}$ is defined by the semi-difference of the voltage drops $\Delta\phi_{m1}$ and $\Delta\phi_{m2}$ in the electrodes. Using the explicit expressions for these quantities and Eq. (5), we find

$$\Delta\bar{\phi} = \frac{c_i t}{2(\varepsilon_0 + c_i t)} P_3 \left(\frac{1}{c_{m2}} - \frac{1}{c_{m1}} \right) \cong \frac{1}{2} P_3 \left(\frac{1}{c_{m2}} - \frac{1}{c_{m1}} \right), \quad (23)$$

where $P_3 = P_3(t)$ is the thickness-dependent equilibrium polarization in the barrier. Equation (23) demonstrates that the depolarizing-field effect on the mean potential is directly proportional to the difference between the reciprocal capacitances of two electrodes. The magnitude of $\Delta\bar{\phi}$ is expected to be large when one electrode is made of a conducting perovskite material like SrRuO₃, whereas the other electrode is produced of an elemental metal like Pt. Accordingly, taking $c_{m1} \approx 0.9$ F/m² [13], $c_{m2} \approx 0.4$ F/m² [24], and estimating P_3 from Fig. 2, we find that at $V_a = (W_1 - W_2)/e$ the change $\Delta\bar{\phi}$ can be as large as 0.2 V in BaTiO₃ films and 0.4 V in Pb(Zr_{0.5}Ti_{0.5})O₃ films.

The depolarizing-field effect on the conductance of a FTJ can be evaluated in the approximation of an average barrier [39,3]. Depending on the polarization orientation in the junction, $\Delta\bar{\phi}$ either increases or reduces the mean barrier height, which leads to the appearance of two different resistance states. When the bias voltage $V_a = (W_1 - W_2)/e$ is small, the ratio of conductances G_L and G_H , which characterize the low- and high-resistance states at $V = V_a$, can be estimated in the linear approximation as

$$\frac{G_L}{G_H} \cong \frac{\left(1 + \frac{t}{t_\varphi} \sqrt{1 - \frac{e|\Delta\bar{\phi}|}{\varphi_0}} \right) \exp\left(-\frac{t}{t_\varphi} \sqrt{1 - \frac{e|\Delta\bar{\phi}|}{\varphi_0}} \right)}{\left(1 + \frac{t}{t_\varphi} \sqrt{1 + \frac{e|\Delta\bar{\phi}|}{\varphi_0}} \right) \exp\left(-\frac{t}{t_\varphi} \sqrt{1 + \frac{e|\Delta\bar{\phi}|}{\varphi_0}} \right)}, \quad (24)$$

where $t_\varphi = h/(4\pi\sqrt{2m_f^*\varphi_0})$, φ_0 is the average barrier height at zero polarization, and m_f^* is the electron effective mass in the barrier, which may differ considerably from the free electron mass m_e [40,41]. At $\varphi_0 = 0.5$ eV, $|\Delta\phi| = 0.1$ V, and $t = 3.2$ nm, for instance, Eq. (24) gives G_L/G_H about 7 for $m_f^* = 0.2m_e$ and about 600 for $m_f^* = 2m_e$. At large bias voltages V_a , the quadratic and cubic terms in the current-voltage dependence should be also taken into account for the correct evaluation of G_L and G_H [3]. For FTJs involving Pt and SrRuO₃ electrodes, e.g., the ratio G_L/G_H at the bias voltage $V_a \approx 0.45$ V appears to be about 9 for $m_f^* = 0.2m_e$ and ~ 900 for $m_f^* = 2m_e$. Thus, the conductance on/off ratio rises steeply with the increase of effective mass.

V. CONCLUSION

In this paper, we have shown that the single-domain polarization state may be stabilized in ultrathin ferroelectric films by compressive in-plane strains counteracting the depolarizing-field effect. The reduction of spontaneous polarization, which is caused by E_{dep} , depends on the total capacitance of the screening charge in the electrodes (but not on their screening lengths as supposed in some recent publications [4,10,12]). In contrast, the depolarizing-field effect on the tunnel current through an ultrathin ferroelectric barrier is predominantly governed by the difference between the reciprocal capacitances of two electrodes.

ACKNOWLEDGMENT

The financial support of the Deutsche Forschungsgemeinschaft is gratefully acknowledged. The research described in this paper was also supported by the Volkswagen-Stiftung project “Nano-sized ferroelectric hybrids” under contract No I/77737.

References

1. J. F. Scott, *Ferroelectric Memories* (Springer, Berlin, 2000).
2. H. Kohlstedt, N. A. Pertsev, and R. Waser, in *Ferroelectric Thin Films X*, edited by S. R. Gilbert, Y. Miyasaka, D. Wouters, S. Trolier-McKinstry, and S. K. Streiffer, MRS Symposia Proceedings No 688 (Materials Research Society, Pittsburg, 2002), p. 161.
3. H. Kohlstedt, N. A. Pertsev, J. Rodríguez Contreras, and R. Waser. *Phys. Rev. B* **72**, 125341 (2005).
4. M. Ye. Zhuravlev, R. F. Sabirianov, S. S. Jaswal, and E. Y. Tsymlal, *Phys. Rev. Lett.* **94**, 246802 (2005).
5. I. I. Ivanchik, *Sov. Phys. Solid State* **3**, 2705 (1962).
6. G. M. Guro, I. I. Ivanchik, and N. F. Kovtonyuk, *Sov. Phys. Solid State* **11**, 1574 (1970).
7. I. P. Batra and B. D. Silverman, *Solid State Comm.* **11**, 291 (1972); I. P. Batra, P. Würfel, and B. D. Silverman, *Phys. Rev. Lett.* **30**, 384 (1973).
8. R. R. Mehta, B. D. Silverman, and J. T. Jacobs, *J. Appl. Phys.* **44**, 3379 (1973).
9. D. R. Tilley and B. Žekš, *Ferroelectrics* **134**, 313 (1992).
10. J. Junquera and Ph. Ghosez, *Nature (London)* **422**, 506 (2003).
11. N. Sai, A. M. Kolpak, and A. M. Rappe, *Phys. Rev. B* **72**, 020101(R) (2005).
12. C. Lichtensteiger, J.-M. Triscone, J. Junquera, and Ph. Ghosez, *Phys. Rev. Lett.* **94**, 047603 (2005).
13. D. J. Kim, J. Y. Jo, Y. S. Kim, Y. J. Chang, J. S. Lee, J.-G. Yoon, T. K. Song, and T. W. Noh, *Phys. Rev. Lett.* **95**, 237602 (2005).
14. R. Kretschmer and K. Binder, *Phys. Rev. B* **20**, 1065 (1979).
15. N. A. Pertsev, A. G. Zembilgotov, and A. K. Tagantsev, *Phys. Rev. Lett.* **80**, 1988 (1998).
16. N. A. Pertsev, V. G. Kukhar, H. Kohlstedt, and R. Waser, *Phys. Rev. B* **67**, 054107 (2003).
17. A. G. Zembilgotov, N. A. Pertsev, H. Kohlstedt, and R. Waser, *J. Appl. Phys.* **91**, 2247 (2002).

18. N. A. Pertsev, J. Rodríguez Contreras, V. G. Kukhar, B. Hermanns, H. Kohlstedt, and R. Waser, *Appl. Phys. Lett.* **83**, 3356 (2003).
19. T. Mitsui and J. Furuichi, *Phys. Rev.* **90**, 193 (1953); A. Kopal, T. Bahnik, and J. Fousek, *Ferroelectrics* **223**, 127 (1999); A. M. Bratkovsky and A. P. Levanyuk, *Phys. Rev. Lett.* **84**, 3177 (2000).
20. A. M. Bratkovsky and A. P. Levanyuk, *cond-mat/0601484*.
21. Ch. Kittel, *Introduction to Solid State Physics* (Wiley, New York, 1996).
22. H. Ehrenreich and H. R. Philipp, *Phys. Rev.* **128**, 1622 (1962).
23. H. Y. Ku and F. G. Ullman, *J. Appl. Phys.* **35**, 265 (1964).
24. C. T. Black and J. J. Welser, *IEEE Trans. Electron Devices* **46**, 776 (1999).
25. H. Y. Fan, *Phys. Rev.* **61**, 365 (1942); J. G. Simmons, *Phys. Rev. Lett.* **10**, 10 (1963).
26. Since Eq. (5) was obtained in the continuum approximation, it involves the work functions W_1 and W_2 of metals with free and clean surfaces. We are aware of the fact that the short-range atomic interactions at the ferroelectric-metal interface could create interfacial states and dipoles. Those may modify the work functions and screening conditions thus changing the electric field distribution in the MFM heterostructure. An advanced microscopic treatment is necessary to evaluate this distribution with a high accuracy.
27. A. L. Roytburd, S. Zhong, and S. P. Alpay, *Appl. Phys. Lett.* **87**, 092902 (2005).
28. Parameters of $\text{Pb}(\text{Zr}_{0.5}\text{Ti}_{0.5})\text{O}_3$ (in SI units, temperature T in $^\circ\text{C}$) used in the calculations: $a_1 = 1.33(T - 392.6)\times 10^5$, $a_{11} = 5.26\times 10^8$, $a_{12} = -1.847\times 10^8$, $a_{111} = 1.336\times 10^8$, $a_{112} = 6.128\times 10^8$, $a_{123} = -2.894\times 10^9$, $c_{11} = 1.545\times 10^{11}$, $c_{12} = 8.405\times 10^{10}$, $c_{44} = 3.484\times 10^{10}$, $q_{11} = 7.189\times 10^9$, $q_{12} = -2.853\times 10^9$, $q_{44} = 2.854\times 10^9$.
29. Y. L. Li, L. E. Cross, and L. Q. Chen, *J. Appl. Phys.* **98**, 064101 (2005).
30. Parameters of BaTiO_3 used in the calculations: $a_1 = 4.124(T - 115)\times 10^5$, $a_{11} = 5.328\times 10^8$, $a_{12} = 3.426\times 10^8$, $a_{111} = 1.294\times 10^9$, $a_{112} = -1.95\times 10^9$, $a_{123} = -2.5\times 10^9$, $a_{1111} = 3.863\times 10^{10}$, $a_{1112} = 2.529\times 10^{10}$, $a_{1122} = 1.637\times 10^{10}$, $a_{1123} = 1.367\times 10^{10}$, $c_{11} = 1.755\times 10^{11}$, $c_{12} = 8.464\times 10^{10}$, $c_{44} = 1.082\times 10^{11}$, $q_{11} = 1.203\times 10^{10}$, $q_{12} = -1.878\times 10^9$, $q_{44} = 6.385\times 10^9$.
31. E. V. Chenskiĭ and V. V. Tarasenko, *Sov. Phys. JETP* **56**, 618 (1982).
32. V. A. Stephanovich, I. A. Luk'yanchuk, and M. G. Karkut, *Phys. Rev. Lett.* **94**, 047601 (2005).
33. The wave vector \mathbf{k} of polarization perturbation is assumed to be parallel to the [100] crystallographic axis. The case of the [110]-oriented \mathbf{k} can be described in a similar way.
34. W. Cao and L. E. Cross, *Phys. Rev. B* **44**, 5 (1991).
35. This estimate was obtained using Eq. (3) and the experimental data of Ref. 13. The same value follows from the results of first-principles calculations performed by G. Gerra *et al.* [*Phys. Rev. Lett.* **96**, 107603 (2006)] for $\text{SrRuO}_3/\text{BaTiO}_3/\text{SrRuO}_3$ capacitors.
36. It should be emphasized that the depolarizing field E_{dep} in the film with $t \neq t_{\text{th}}$ is smaller than the thermodynamic coercive field at a given misfit strain [18].
37. C. Yoshida, A. Yoshida, and H. Tamura, *Appl. Phys. Lett.* **75**, 1449 (1999).
38. H. B. Michaelson, *IBM J. Res. Dev.* **22**, 72 (1978).
39. J. G. Simmons, *J. Appl. Phys.* **34**, 1793 (1963).
40. C. N. Berglund and W. S. Baer, *Phys. Rev.* **157**, 358 (1967).
41. M. Dawber, K. M. Rabe, and J. F. Scott, *Rev. Mod. Phys.* **77**, 1083 (2005).